

Piezoelectricity, Pyroelectricity, and Thermoelectricity of Polymer Films

TAKEO FURUKAWA, YUTAKA UEMATSU,
KIYOSHI ASAKAWA, and YASAKU WADA, *Department of
Applied Physics, Faculty of Engineering, University of Tokyo,
Bunkyo-ku, Tokyo, Japan*

Synopsis

Some electrical phenomena in amorphous and partially crystalline polymers are studied. The phenomena are phenomenologically similar to those in crystalline materials, but their origin is concluded to be space charges embedded in polymers. Voltage is induced across the surfaces of polymer films, i.e., polystyrene, poly(methyl methacrylate), polyethylene, and polypropylene, when they are vibrated in elongation (elongational piezoelectricity) and in bending (bending piezoelectricity). The former is attributed to a space charge distribution which is antisymmetrical about the median plane of the film and the latter to symmetrical distribution. A general description of piezoelectricity of a system in which space charge is embedded in homogeneous continuum is developed. Output current from poly(vinyl chloride) films at high temperatures (above 125°C) was measured under the following conditions: (1) under potential gradient (electrical conduction), (2) under temperature gradient (thermoelectricity), and (3) when the film is uniformly heated (pyroelectricity). Pyroelectricity is attributed to drift of space charge to electrodes on account of electrostatic force by image charge. Depolarization current of a poly(vinyl chloride) film which has been polarized at 125°C prior to measurement (electret) is interpreted in terms of dipole disorientation plus space charge drift.

Introduction

Polymeric materials are usually electrically nonconductive at low temperatures but they exhibit some conductivity at high temperatures where macrowebian motion of molecules is allowed. Conductivity is believed to result from migration of ions which are included in the material. The ions may be low molecular impurities and/or polymer molecules themselves. Semiconducting polymers and the high-field, non-ohmic conductivity of polymers are beyond the scope of this study.

Polymeric films, including amorphous and polycrystalline polymers, are usually macroscopically isotropic or, when they are stretched, anisotropic in the plane of film but still isotropic in the thickness direction. The distribution of ions, however, may be inhomogeneous in the film plane and at the same time in the thickness direction. We take herein the x axis as the thickness direction and $x = 0$ at the median plane of the film. Any

distribution of space charge in the film as a function of x may be resolved into two components, a symmetrical function about $x = 0$ and an antisymmetrical one.

The present paper is concerned with preliminary experiments on several electrical phenomena observed in polymer films including ions or space charge. Some of the phenomena are expected in films of symmetrical distribution of charge, some in those of antisymmetrical distribution, and others in both.

It is to be noted that terms in this paper have a broader definition than usual. Polarization means not only microscopic dipole polarization but also macroscopic polarization due to space charge pairs. The output current comes from variation of polarization in the polymer with time. Piezoelectricity means here the polarization change with either uniform or nonuniform strain; pyroelectricity, the polarization change with temperature; thermoelectricity and electrical conduction means current due to temperature gradient and potential gradient in the polymer, respectively.

Piezoelectricity of Polymers in Elongation

Some polymer crystals which belong to space groups without symmetry center exhibit piezoelectricity.¹ Examples are cellulose, protein, and so on. Piezoelectricity of such materials has been well studied for a polycrystalline sample in which crystallites are uniaxially oriented.^{2,3}

In the present study, however, piezoelectricity of polymers which are either amorphous or polycrystalline with randomly oriented lamellae will be discussed. Such a material would show piezoelectricity for elongation along the y axis in the film plane if the space charge distribution has an antisymmetrical component about $x = 0$.

Specimens as listed in Table I were prepared by pressing a commercial pellet between hot metallic plates. The area was 5×5 cm² and the thickness was 0.5 mm. A carbon powder paste (Aquadac) was employed

TABLE I
Piezoelectricity of polymers^a

| | Capacitance C_s , pF | Piezoelectricity | | | |
|--------------------------------|---------------------------|-----------------------------------|--|--|-----------------------------|
| | | Elongation $\Delta V/s$, V | Bending $\Delta V/(l/R)$, 10^{-4} , V-m | e , 10^{-4} , C/m ² | g , 10^{-3} , C/m |
| Polypropylene | 25 | 17.5 | 14.2 | 1.89 | 3.01 |
| Polyethylene (high density) | 23 | 13.5 | 14.1 | 1.58 | 3.25 |
| Polyethylene (low density) | 22 | 6.5 | 9.7 | 0.80 | 2.34 |
| Polystyrene | 28 | 3.8 | 3.4 | 0.37 | 0.64 |
| Poly(methyl methacrylate) | 37 | 0.9 | 2.4 | 0.07 | 0.34 |

^a Electrode area, 2.5×2.5 cm².

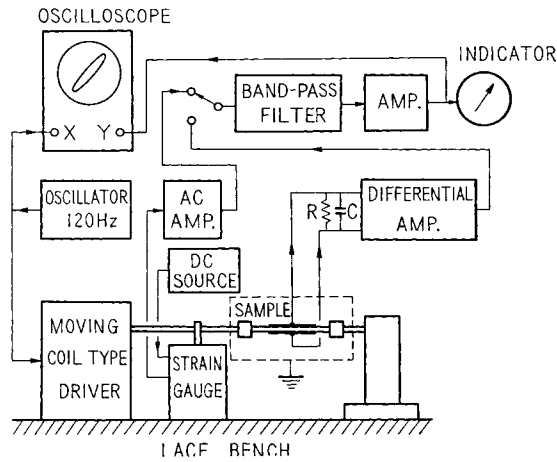


Fig. 1. Schematic representation of apparatus for elongational piezoelectricity.

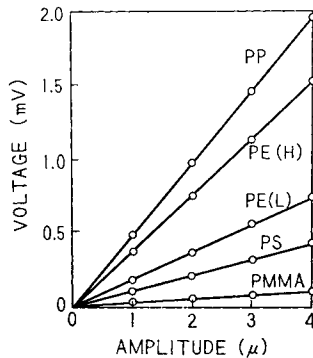


Fig. 2. Induced ac voltage plotted against amplitude of elongation at the end of film. Span length = 3.6 cm; electrode area = $2.5 \times 2.5 \text{ cm}^2$; film thickness = 0.5 mm.

as an electrode material. The electrode dimensions were $2.5 \times 2.5 \text{ cm}^2$. Several electrode materials were tested, and Aquadac was found to be the best. The electrode was so thin that its mechanical resistance to deformation of the specimen was negligible. Thin silver foils, 1 mm in width, were employed as electrical leads from the electrodes.

The apparatus for measuring elongational piezoelectricity is schematically illustrated in Figure 1. The specimen was clamped at one end and sinusoidally driven at the other end along the y axis by a moving-coil driver with a frequency of 120 Hz. The displacement was measured by a resistance strain meter. The span length of the specimen was 3.6 cm.

The induced voltage was amplified by a differential amplifier (gain = 60 db, frequency band = 80–250 Hz) in order to eliminate in-phase noise across two electrodes and then filtered by a narrow-band amplifier tuned to 120 Hz. An oscilloscope served as a detector of phase relation between strain and polarization. All the measurements were made at

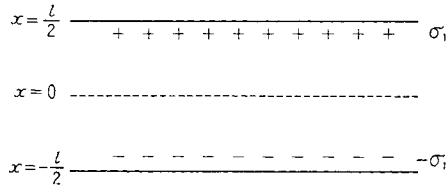


Fig. 3. Simplest model of antisymmetrical space charge distribution in the film.

room temperature. The relation between voltage and strain was linear in each specimen, as shown in Figure 2.

There are some other possibilities for voltage occurrence besides piezoelectricity. If a charge exists on the surface of specimen, the voltage might be induced because electrodes vibrate in the electric field by this charge. Actually, when the surface of the specimen had been rubbed prior to measurement, a large voltage was observed. However, the voltage decayed to the original value after several hours. Another possibility is a thermoelectric effect in the input circuit. The dc electromotive force in the input circuit might be converted to ac power because the capacitance of the specimen varies sinusoidally. These effects were carefully avoided throughout the experiment.

The results are interpreted here in terms of antisymmetrical distribution of space charge in the following. The simplest model for such a distribution is illustrated in Figure 3, in which opposite charges are distributed in the planes $x \pm l/2$, respectively. When the specimen is elongated along the y axis by the strain S , the charge per unit area changes from the original value σ_{10} to $\sigma_1 = \sigma_{10}(1 - S)(1 + mS)$, where m is Poisson's ratio. Then the change of polarization ΔP is given for $S \ll 1$ by

$$\Delta P = - (1 - m)\sigma_{10} S \quad (1)$$

The piezoelectric strain constant e is then written as

$$e = - (1 - m)\sigma_{10} \quad (2)$$

The voltage amplitude ΔV induced across both surfaces of specimen is related to strain amplitude S by

$$\Delta V = \Delta \left(\frac{A\sigma_1}{C + C_s} \right) = - \frac{A\sigma_1 \Delta C_s}{(C + C_s)^2} \simeq - \frac{A\sigma_{10} C_s}{C^2} S \quad (3)$$

because C and $A\sigma_1$ are constant in the present experiment. In eq. (3), A is the electrode area, C_s the capacitance of the specimen, and C is the input capacitance of measuring circuit. In deriving eq. (3), we assume the conditions $C \gg C_s$ and $\omega CR \gg 1$ (where ω = angular frequency of vibration, R = input resistance), which are satisfied through the experiment ($C = 500$ pF, $R = 20$ M Ω , $C_s < 40$ pF). According to the model in Figure 3, the piezoelectric constant e is related to the ratio $(\Delta V/S)$ by

$$e = [C^2 (1 - m)/AC_s] (\Delta V/S) \quad (4)$$

Values of e calculated from the slope of the ΔV versus S plot are given in Table I. The Poisson ratio was taken as $1/3$ for each sample. The data were quite reproducible for the same specimen, but varied from specimen to specimen for the same polymer. Since the value of e is 10^{-4} C/m² in order of magnitude, from eq. (2), σ_{10} should have the magnitude of 10^{-4} C/m².

The space charge in the polymer film may be inhomogeneously distributed along the x axis. The distribution may be divided into two components, one symmetrical around the plane $x = 0$ and the other antisymmetrical. The former does not contribute to the piezoelectricity in the present case. The origin of the antisymmetrical distribution may be, for example, the temperature gradient which the film has undergone during casting. Ions may be moved by thermal osmotic force in the course of casting and assume an antisymmetrical distribution. Two specimens of polyoxymethylene were studied, one of which was pressed in the usual way (a small temperature gradient may exist in this case), and the other pressed under an exaggerated temperature gradient. The value of e of the latter was twice as large as that of the former.

Piezoelectricity of Polymers in Bending

As has been discussed in the last section, only antisymmetrical distribution of space charge contributes to piezoelectric polarization in elongation. For nonuniform strain, however, symmetrical distribution is to be taken into account (see Appendix).

The apparatus for measuring bending piezoelectricity was essentially similar to that for elongational piezoelectricity except for the position of the specimen (Fig. 4). The same specimens as in elongational piezoelectricity were used. Plots of ΔV against the amplitude of upper end x_0 were linear in all cases, as illustrated in Figure 5.

Figure 6 represents the simplest model of symmetrical distribution of charge. If the specimen is fixed at the lower end and driven along the

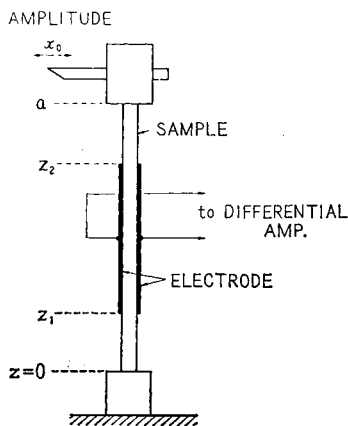


Fig. 4. Geometry of specimen film in bending piezoelectricity measurement.

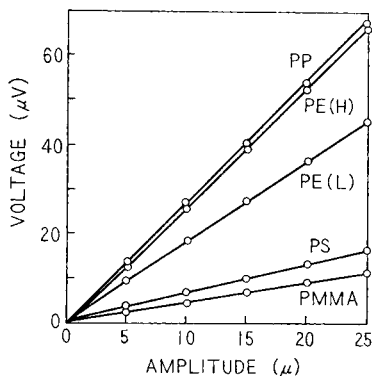


Fig. 5. Induced ac voltage plotted against amplitude at the upper end of film. Span length = 4 cm; electrode area = 2.5×2.5 cm²; film thickness = 0.5 mm.

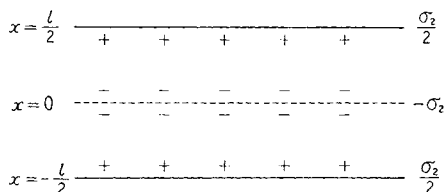


Fig. 6. Simplest model of symmetrical space charge distribution in the film.

x axis at the upper end (bending), one half of the specimen ($x > 0$) is elongated and the other half ($x < 0$) is compressed, or vice versa. Polarization ΔP along the x axis is then calculated for the model in Figure 6, by an equation derived similarly to eq. (1):

$$\Delta P = [\sigma_{20} l (1 - m)/4] (1/R) \quad (5)$$

where R is the radius of curvature. If we define a higher-order piezoelectric constant g as $\Delta P = g(\partial S/\partial x)$ where $(\partial S/\partial x)$ is the strain gradient, (i.e., curvature in this case), g is written as

$$g = \sigma_{20} l (1 - m)/4 \quad (6)$$

Since the curvature changes along the z axis in bending, we must use the average curvature $\langle 1/R \rangle$ over the electrode area from z_1 to z_2 (Fig. 4). Calculation leads to the equation,

$$\langle 1/R \rangle = (3x_0/a^3) [a - 1/2 (z_1 + z_2)] \quad (7)$$

Finally the measured voltage ΔV across the electrodes is given in the same way as eq. (3) by

$$\Delta V = (Al \sigma_{20} C_s/8C^2) \langle 1/R \rangle \quad (8)$$

and g is related to the ratio $\Delta V/\langle 1/R \rangle$ as

$$g = [2C^2 (1 - m)/AC_s] (\Delta V/\langle 1/R \rangle) \quad (9)$$

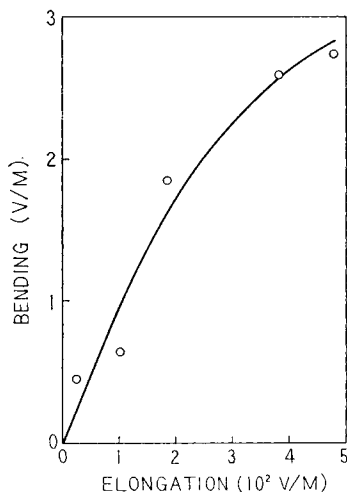


Fig. 7. Correlation between elongation piezoelectricity and bending piezoelectricity, expressed by induced ac voltage divided by amplitude of the end.

Values of g calculated from the ratio are listed in Table I. Since g is 10^{-8} C/m in order of magnitude, σ_{20} is estimated at 10^{-4} C/m² from eq. (6), being of the same order as σ_{10} obtained from elongational piezoelectricity.

Figure 7 represents the correlation between two types of piezoelectricity, where one can see that specimens with a large e value have a large g value, too. This is quite natural, because specimens with a large amount of space charge may have large values of both σ_{10} and σ_{20} .

According to Kogan,⁴ piezoelectricity due to strain gradient should be observed in crystal with symmetry center. In crystals of NaCl type, for example, g (or more strictly speaking, a component of the g tensor) is equal to $e/8a$, where e is the ion charge and a the lattice spacing. In polyethylene crystals which belong to the space group D_{2h}^{16} (orthorhombic system), g should have a nonzero component even if no space charge exists. The value is, however, too small to permit interpretation of the observed value of g because of the small dipole moment of the C—H bond.

Electrical Conductivity and Thermoelectricity of Polymers

When the temperature of polymers becomes sufficiently high, the space charge can be moved by an external force. Electrical current in usual polymers at high temperatures is believed to result from this effect.

Figure 8 represents the logarithm of electrical resistance against reciprocal absolute temperature of poly(vinyl chloride). The specimen was cut from a commercial rigid PVC film, including no plasticizer. The thickness was 0.2 mm and the electrode area was 4.5×4.5 cm². Aluminum foils were employed as electrodes. The resistance was measured with an ac bridge at 30 Hz to avoid the depolarization effect. The heating rate was 2.0°C/min. The value of resistance was somewhat scattered among speci-

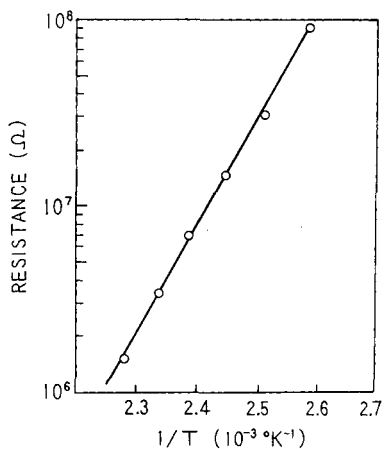


Fig. 8. Electrical resistance of PVC film plotted against temperature. Electrode area = 4.5×4.5 cm²; film thickness = 0.2 mm; heating rate = 2.0°C/min.

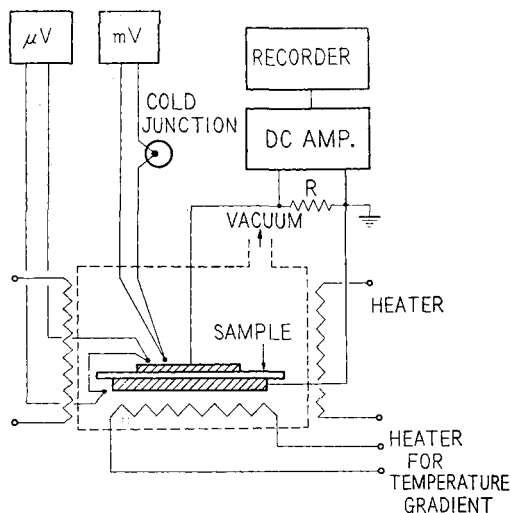


Fig. 9. Schematic representation of apparatus for measuring thermoelectricity and pyroelectricity. Heater for temperature gradient used only in thermoelectricity measurement.

mens which were cut from the same original film, but the temperature dependence was quite similar as long as the heating rate was sufficiently high.

Assuming a single species of carrier for simplicity, the conductivity κ is expressed by

$$\kappa = nq\mu \quad (10)$$

where n is the carrier density, q the charge of a carrier, and μ the mobility. The activation energy H obtained from the slope in Figure 8 may be equal

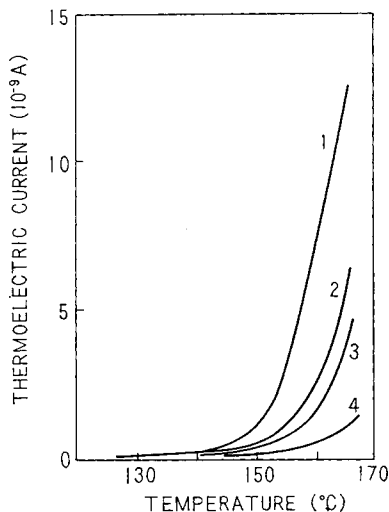


Fig. 10. Thermoelectric current of four specimens of PVC film plotted against temperature of lower-temperature side. Electrode area = $4.5 \times 4.5 \text{ cm}^2$; film thickness = 0.2 mm; heating rate = $2.0^\circ\text{C}/\text{min}$; temperature difference = 13°C .

to that of μ if n is assumed constant during measurement. This assumption may be valid in this case, because the heating rate was sufficiently high, as will be discussed in the following section. The value of H is calculated as 27 kcal/mol from Figure 8, being comparable with the activation energy of viscous flow in this material as estimated from Williams-Landel-Ferry's equation.⁵ This is reasonable because carriers drift in the viscous medium.

Carriers in the polymer are also expected to move by temperature gradient (thermoelectricity). The apparatus for measuring thermoelectricity is sketched in Figure 9. Examples of results are drawn in Figure 10, which were measured for a 13°C difference between the two electrodes. The current in the load R was always positive (from high-temperature side to low-temperature side in the specimen). Temperature variation of current is similar to that of electrical conductance, indicating thermoelectromotive force does not depend on temperature so much when the temperature difference is kept unchanged.

The value of thermoelectric current varied from specimen to specimen, reflecting the difference of charge density. Another reason for this variation may be the pyroelectricity of this material, the polarity of which varies from sample to sample, as will be fully described in the following section. The specimen with positive pyroelectricity may show a strong thermoelectric current but that with negative pyroelectricity may show a weak current, on account of cancellation of the two phenomena.

Pyroelectricity of Polymers

When the polymer film is uniformly heated, an electric current is observed in the load resistance. This phenomenon is termed pyroelectricity.

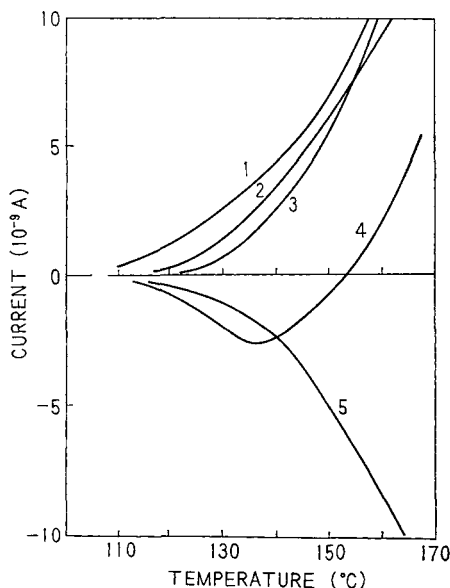


Fig. 11. Pyroelectric current of five specimens of PVC film plotted against temperature. Electrode area = $4.5 \times 4.5 \text{ cm}^2$; film thickness = 0.2 mm; heating rate = $2.0^\circ\text{C}/\text{min}$.

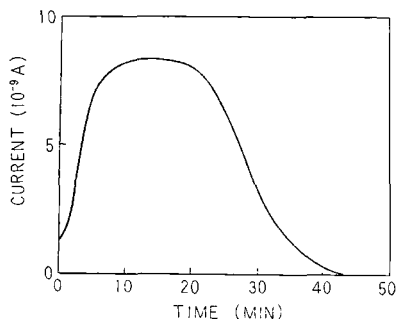


Fig. 12. Pyroelectric current of PVC specimen at 165°C plotted against time. Electrode area = $1.3 \times 1.3 \text{ cm}^2$; film thickness = 0.5 mm; specimen heated to 165°C at the rate of $6^\circ\text{C}/\text{min}$.

The arrangement for measurement of pyroelectricity of polymer films was essentially similar to that for measurement of thermoelectricity, except that the temperature of the specimen was uniform and no temperature gradient was applied. Specimens were also the same as those in the last section, i.e., rigid poly(vinyl chloride). Al foils and vacuum-deposited Ag films were used for electrodes, but no appreciable difference was found in results between them. The current was recorded as a function of time with a constant heating rate. In some experiments, the specimen was heated to a definite temperature as fast as possible and kept at the temperature. Results are summarized as follows.

The current starts at about 125°C (Fig. 11). The smaller current is observed for the higher heating rate. The current is observed for several

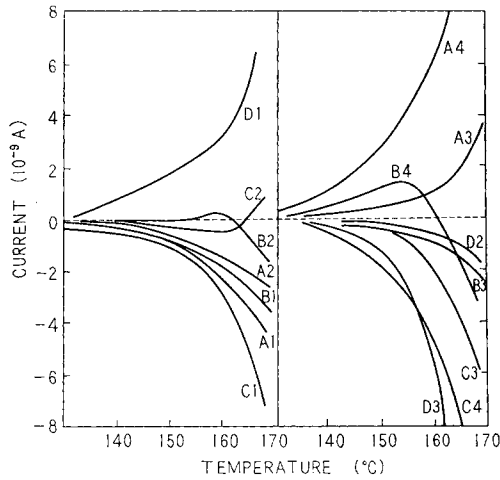


Fig. 13. Pyroelectric current of 15 specimens of PVC film cut out from a sheet as indicated in Fig. 14. Electrode area = $1 \times 1 \text{ cm}^2$; film thickness = 0.2 mm; heating rate = $6^\circ\text{C}/\text{min}$.

| | A | B | C | D |
|---|---|---|---|---|
| 1 | - | - | - | + |
| 2 | - | ± | ∓ | - |
| 3 | + | - | - | - |
| 4 | + | ± | - | |

1.3MM

Fig. 14. Arrangement of 15 specimens in Fig. 13 in the original sheet. Signs in the figure represent polarity of pyroelectricity. ± (or ∓) means current first positive then negative (or vice versa).

heating cycles when the rates of heating and cooling are sufficiently high. When the specimen is held at a constant temperature, the current increases first, goes through maximum, and then tends to zero (Fig. 12). No current is observed for the specimen which has been heat-treated for a long time and then cooled.

The polarity of the current changes from place to place in the original film. Figure 13 represents results for 15 pieces of specimen cut from a film as indicated in Figure 14. The range of inhomogeneity is in the order of 1 cm. The amount of current does not depend so much on the area of specimen, probably because of the cancellation of currents from different places in the specimen.

The output current is independent of load resistance R , as far as R is much smaller than the resistance of the specimen. This would mean that the film is not a voltage source but a current source.

When two mica sheets (thickness = 0.2 mm) are inserted between the specimen and two electrodes, no current is detected.

The phenomena are quite similar in air and *in vacuo*.

The pyroelectricity of the polymer film described above seems to be well interpreted, qualitatively at least, on the assumption of antisymmetrical distribution of space charge in the film. A simple model is illustrated in Figure 15, which represents a space charge Q embedded in the specimen. When electrodes on both surfaces of the film are short-circuited, counter charges $-Q'$ and $-Q''$ are induced on the electrodes, respectively,

$$\begin{aligned} Q' &= Q [(l/2) + x]/l \\ Q'' &= Q [(l/2) - x]/l \end{aligned} \quad (11)$$

where l is the film thickness and x the position of charge Q .

The electrostatic force F on Q by these image charges is an odd function of x . The force is positive or negative when x is positive or negative, respectively, and the charge is pulled towards the nearest electrode. The output current I is then given by

$$I = dQ'/dt = -dQ''/dt = (Q/l) dx/dt \quad (12)$$

and if all the carrier ions are assumed to undergo the force F , for simplicity,

$$I = (Q\mu/lq)F \quad (13)$$

where μ and q are the mobility and charge of a carrier. The current I increases with increasing temperature because of the increase in μ , but finally vanishes when the charge approaches the electrode. When the heating rate is high enough and hence the displacement of the charge during the experiment is small, F may be approximately constant, and the increase in I with temperature reflects mostly the increase in μ . In fact, a plot of $\log I$ against $1/T$ gave the same activation energy as that of electrical resistance in Figure 8.

The integrated current Q^* becomes

$$Q^* = \int_0^\infty |I| dt = \begin{cases} \frac{(l/2) - x_0}{l} Q & x_0 > 0 \\ \frac{(l/2) + x_0}{l} Q & x_0 < 0 \end{cases} \quad (14)$$

where x_0 is the position of charge at $t = 0$. The value of Q^* was calculated as 10^{-6} to 10^{-5} coulomb (area $\simeq 1$ cm²), which is too large to attribute the current to dipole disorientation.

In some cases, the current was first negative then turned to positive (or vice versa) with increasing temperature or with elapse of time. This may be explained if two charges are assumed, one at $x_0 < 0$ near the surface and the other at $x_0 > 0$ near the median plane. Since the absolute value of F becomes very large near the surface ($|F| \propto (l/2 + x)^{-2}$ when $x \simeq -l/2$), the former charge can move at lower temperatures at which μ is small. The

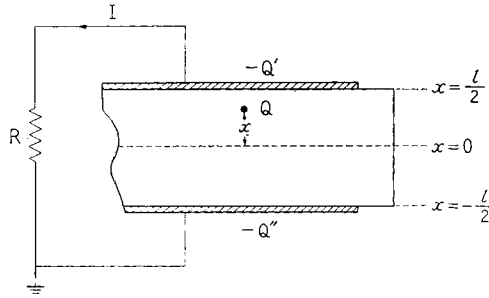


Fig. 15. Simple model for interpreting pyroelectricity of polymer film. A point charge Q embedded at x in the film.

integrated current Q^* for the former part is small as expected from eq. (14).

When the specimen is sandwiched between mica films, the force towards $x = 0$ acts on Q on account of lower dielectric constant of mica than poly(vinyl chloride) at the temperature of experiment. The value of $|F|$ is small in this case, resulting in a small current in the load resistance.

Depolarization of Electret

A polymer film with an antisymmetrical charge distribution has a persistent polarization and may be termed an electret. An electret is prepared by quenching polymer films under high dc voltage.⁶ Electrets were made in the above process from poly(vinyl chloride) films similar to those used in pyroelectricity measurement. The specimen had a thickness of 0.37 mm and electrode area of $4 \times 4 \text{ cm}^2$. The specimen was applied to a dc field of $1.5 \times 10^6 \text{ V/m}$ at 125°C and then quenched.

An example of depolarization current is represented in Figure 16, where the current goes from the electrode which was positive in charging (heterocharge electret). The initial current up to 50°C (current A) may result from desorption of ions from the film surface. The current from 50 to

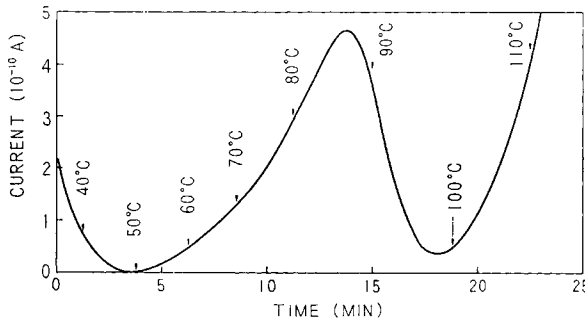


Fig. 16. Depolarization current of electret of PVC. Electrode area = $4 \times 4 \text{ cm}^2$; film thickness = 0.37 mm; polarization was made by electric field $1.5 \times 10^6 \text{ V/m}$ at 125°C for 45 min and then quenched.

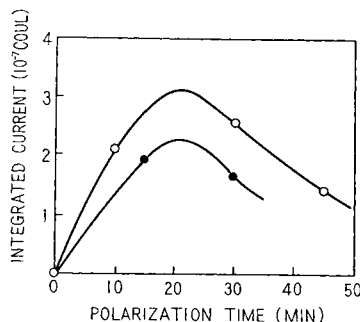


Fig. 17. Integrated depolarization current from 50 to 100°C plotted against polarization time: (O) data just after polarization; (●) 1 day after polarization.

100°C (current B) is characteristic of the electret. The current above 100°C (current C) is essentially similar to pyroelectric current described in the last section and the polarity is not always the same as B, depending on the specimen. Figure 17 represents the integrated value Q^* of depolarization current B plotted against the polarization time.

There are various opinions on the mechanism of electret formation.⁶ Some authors attribute the polarization to dipole orientation and some to the space charge. Assuming free dipole orientation, the dipole polarization P_d by the electric field E is written as⁷

$$P_d = N\mu L(\mu E/kT) \quad (15)$$

where N is the dipole density, μ the dipole moment, and L the Langevin function. Using the numerical values $\mu = 2.2$ D (moment of $-\text{CH}_2-\text{CHCl}-$ unit), $N = 1.3 \times 10^{22}/\text{cc}$, $E = 1.5 \times 10^6 \text{V/m}$, and $T = 350^\circ \text{K}$, we obtain $P_d = 8 \times 10^{-5} \text{coulomb/m}^2$, which has the same order of magnitude as the observed Q^* value.

The curves in Figure 17 show that Q^* increases first with increasing polarization time, then decreases. The time dependence of Q^* of this type may not be interpreted by the dipole orientation alone, and the effect of space charge introduced from the electrodes is to be considered.

APPENDIX

A general formulation of piezoelectricity of the system in which n ions with electric charge q_k ($k = 1, 2, \dots, n$) are embedded in a homogeneous continuum is described in the following.

In such a system, displacement u_α of ions may be similar to external, macroscopic strain $u_{\alpha\beta}$, that is,

$$u_\alpha(k) = \sum_\beta u_{\alpha\beta} x_\beta(k) \quad (15)$$

where the subscripts α, β, γ stand for cartesian coordinates (1,2,3) and $x(k)$ is the position of the k th ion. When strain is not uniform but a function of position, it is expanded as

$$u_{\alpha\beta} = (u_{\alpha\beta})_0 + \sum_{\gamma} \left(\frac{\partial u_{\alpha\beta}}{\partial x_{\gamma}} \right)_0 x_{\gamma} + \dots \quad (16)$$

Then the polarization P_{α} becomes

$$P_{\alpha} = \sum_k q_k u_{\alpha}(k) = \sum_{\beta} (u_{\alpha\beta})_0 e_{\beta} + \sum_{\gamma} \sum_{\gamma} \left(\frac{\partial U_{\alpha\beta}}{\partial x_{\gamma}} \right)_0 g_{\beta\gamma} + \dots \quad (17)$$

where

$$e_{\beta} = \sum_k q_k x_{\beta}(k) \quad (18)$$

and

$$g_{\beta\gamma} = \sum_k q_k x_{\beta}(k) x_{\gamma}(k) \quad (19)$$

It is easily seen that e_{β} is the dipole moment of the system, $g_{\beta\gamma}$ the quadrupole moment, and so on.

It is generally concluded that, for a system in which charges are displaced similarly to macroscopic strain, the first-order piezoelectricity (piezoelectricity due to uniform strain) appears only when the system has a dipole moment but higher-order piezoelectricity due to nonuniform strain should be observed if the system has a multipole moment.

The authors are gratefully indebted to Dr. E. Fukada and Dr. K. Okano for valuable suggestions. They also acknowledge the assistance of Mr. H. Hirose, who prepared the poly(vinyl chloride) film, Mr. M. Matsui and Mr. K. Inoue, who obtained part of the data, and Miss Y. Inoue who prepared the manuscript of the paper.

References

1. W. G. Cady, *Piezoelectricity*, McGraw-Hill, New York, 1946.
2. E. Fukada, *J. Phys. Soc. Japan*, **10**, 149 (1955).
3. E. Fukada and I. Yasuda, *Japan. J. Appl. Phys.*, **3**, 117 (1964).
4. S. M. Kogan, *Soviet Phys.-Solid State*, **5**, 2069 (1964).
5. M. L. Williams, R. F. Landel and J. D. Ferry, *J. Amer. Chem. Soc.*, **77**, 3701 (1955).
6. M. L. Miller, *J. Polym. Sci. A-2*, **4**, 685 (1966).
7. H. Fröhlich, *Theory of Dielectrics*, Oxford Univ. Press, London, 1958.

Received May 8, 1968